STUDY OF FLAME RESPONSE TO SELF EXCITED AND FORCED ACOUSTIC PERTURBATIONS USING LASER DIAGNOSTICS

Frithjof Scheel, Sara Gashi, Clemens Kaminski
University of Cambridge, Department of Chemical Engineering, Pembroke Street, Cambridge CB2 3RA, UK

Ann Dowling
University of Cambridge, Department of Engineering, Trumpington Street, Cambridge CB2 1PZ, UK

ABSTRACT

Combustion oscillations that arise in gas turbines can lead to plant damage. One method used to predict these oscillations is to analyze the acoustics using a simple linear model. This model requires a flame transfer function to describe the response of the heat release to flow perturbations. Laser Induced Fluorescence (LIF) of OH radicals and OH emission has been used to analyze the response of a lean premixed flame to oncoming flow perturbations. Both self-excited oscillations and low amplitude forced oscillations at various frequencies are investigated in an atmospheric combustion rig. In order to visualize fluctuations of local fuel distribution Acetone-LIF is applied as well in non reacting and forced oscillation flow conditions. Various options of image acquisition are successfully applied which include mainly taking a series of images at one particular phase angle of the oscillation over successive pressure cycles and time resolved series of images around one phase angle with time steps as short as 10 μs. This paper focuses on one oscillation frequency, 200 Hz, and the analysis of phase angle locked images. Comparative experiments show that the flame and the combustion intensity develop likewise throughout the pressure cycle of the acoustic oscillation but the maximum fluorescence intensities differ substantially. Nevertheless, these results encourage a comparison of the OH-LIF and the Acetone-LIF results. Quantitative measurements of the equivalence ratio in specific areas of the imaged plane offer explanations to the coupling of the flow oscillation and the combustion oscillation. These confirm the assumption of a coupling of acoustic perturbations, i.e. flow velocity fluctuations, fuel distribution and combustion intensity to be the driving force behind the self excited combustion oscillation.

NOMENCLATURE

Symbols

D	diameter
l	length
$\dot{m}$	mass flow
N	number density
p	pressure
$S_\lambda(T)$	correction factor for Acetone-LIF signal quantification
T	temperature
Δ	difference (general)
Φ	equivalence ratio
Φ_{LIF}	fluorescence yield
ν	frequency

Subscripts

Ac	acetone-related
air	air-related
Exc	related to transition excitation
fuel	fuel-related

Superscript

0	reference condition

Abbreviations

AOI	area of interest (imaged area)
c/c	combustion chamber
e/r	equivalence ratio
f/o	forced oscillation
p/t	pressure transducer
SEO	self excited oscillation

1. INTRODUCTION

Control of combustion instabilities has become a major issue in the design of industrial gas turbines aero engines. Emissions regulations have forced manufacturers to operate lean and premixed, which allows a substantial reduction of NO_x and other harmful emissions from gas turbine engine exhausts to be achieved. However, these operating conditions are particularly susceptible to thermo-acoustic instabilities which are well-known to cause significant damage and hence expensive down-time for the end user [1-3]. Solutions are almost always retro-fitted, since prediction of these instabilities is difficult and are generally only diagnosed during full-scale engine testing. With the EU guideline to decrease NO_x emissions from aero engines by 80 % in the near future the investigation of lean premixed combustion has become a major issue in engine development. The project INTELLECT D.M. (Integrated Lean Low Emission Combustor Design Methodology) is aimed to increase the data base on lean premixed combustion and the resulting effects in order to finally allow the development of design tools which will enable the designer to predict and thus prevent the occurrence of self excited combustion oscillation already in the design phase the engine.

Dowling & Stow [4] applied wave–propagation analysis techniques in which the linearised continuity, momentum equation(s) and the energy equation are used to analyze the stability and frequency characteristics of simplified combustion systems. The form of the flame model, which represents the unsteady combustion in such an analysis, is crucial in determining the predicted response of a given combustor configuration. The flame model usually takes the form of a transfer function, relating the response of the heat release to oncoming flow perturbations. The flow perturbations that are most significant are determined by the characteristics of the combustion system under investigation. Currently a number of analytical flame models have been published in the literature, a summary of which can be found in Dowling [5]. However, so far there is no physical model of a lean, premixed flame that predicts the reported response of simple experimental flames [6].

The mechanism producing these self excited instabilities is an interaction between unsteady combustion and acoustic waves. According to Rayleigh [7], if the rate of heat addition and the acoustic waves are in phase, the heat addition amplifies the acoustic waves and self-excited oscillations can occur. In gas turbines this basic mechanism has been seen to occur in various forms, leading to 'buzz' in afterburners [8] and low frequency 'rumble' in aero engine combustors at idle/sub-idle conditions [9]. The accepted mechanism for instability in lean premixed combustion in turbines is that small pressure fluctuations can produce resultant fluctuations in the air flow entering the premix ducts. This in turn produces small changes in the equivalence ratio which, near the lean limit, lead to appreciable variations in the combustor reaction rate [10]. Amplification occurs when these variations in the combustor reaction rate reinforce the pressure oscillations. This can result in significant damage to the combustor and hence limit the operational envelope of the gas turbine or engine. The aim the presented experiments is to increase the insight into the coupling of involved flow parameters and the combustion intensity. OH LIF is applied to provide flame front and qualitative combustion intensity data with high spatial and temporal resolution in a defined plane. Acetone LIF is applied to measure the space and time resolved quantitative equivalence ratio distribution during the pressure cycle of the flow perturbation. Although the latter can only be applied reliably in non-reacting flow it may well lead to a better understanding of the processes in the combustion chamber.

2. EXPERIMENTAL SET UP

2.1. The test rig

The facility is a generic combustor designed to model the premix ducts of a Rolls–Royce RB211–DLE industrial gas turbine. The swirler unit is a scale model. However, the geometry of the plenum and combustor has been reduced to simple cylindrical pipes. This is because their influence on the combustion system may be quantified provided the experimental set up has well-defined acoustic boundary conditions. The experiments are carried out under atmospheric conditions. A schematic view of this so called buzz rig is given in FIG. 1.

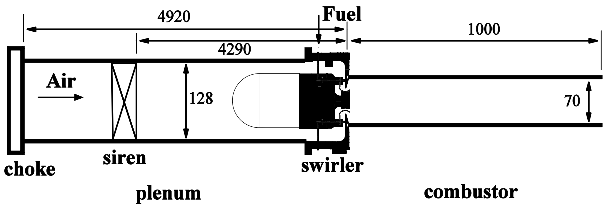

FIG. 1. Schematic view of the buzz rig

A metered and steady air flow is supplied to the plenum through a choked plate to decouple the air supply from pressure fluctuations in the working section (plenum and combustor). The air mass flow rate for these experiments is $\dot{m}_{air}$=0.044 kg/s. For the forced oscillations a siren is placed downstream of the choke plate which produces pressure fluctuations in the working section (see Armitage et al. [6] for details of the siren). For the self-excited oscillations, the siren is removed and the choked plate is placed 1800 mm from the front face of the swirler unit.

The downstream end of the plenum chamber incorporates an annular section prior to the swirler unit. The swirler exit is connected to a quartz tube along which combustion takes place. This provides good optical access to the flame region. The exit of the tube is open to atmospheric pressure. The fuel (ethylene, C_2H_4) and air are mixed using a Rolls-Royce DLE counter-rotating, radial swirler unit, scaled to fit the existing facilities (approx. 54%), shown in FIG. 2. Fuel injection occurs through 8 cylindrical fuel bars mounted inside the swirler unit.

A pressurized commercial cylinder is used to supply the fuel for the swirler unit. The fuel line comprises a pressure regulator, control valve and turbine-flow meter. Together with suitably located pressure transducers and thermocouples, the turbine-flow meter is used to provide a mass-flow reading. The fuel mass flow rate $\dot{m}_{fuel}$ and the resulting equivalence ratio Φ determine the frequency at which self excited oscillations occur - if so at all. With $\dot{m}_{fuel}=1.8\cdot10^{-3}$ kg/s and a resulting equivalence ratio of Φ=0.6 a self excited oscillation with a frequency of ν_{SEO}=200 Hz is obtained. The air mass flow rate, the equivalence ratio and the geometric configuration (including the fuel bars) are all used to define the operating points of the combustor rig. Identical flow parameters have been applied to experiments with forced oscillations.

A Kistler piezo–electric pressure transducer (type 601A) measures the combustor pressure at a location 700 mm downstream from the swirler front face. This pressure signal is used to trigger the LIF system in the self-excited oscillations experiments. When the flame is forced using the siren, the LIF system is triggered using the encoder feedback from the motor that drives the siren. The transducer is located in a side arm, 30mm from the combustor wall. The semi–infinite line technique [14] is used to provide adequate thermal isolation from the hot combustion products, while also ensuring that the pressure signal at the transducer is not distorted by reflecting waves.

2.2. The laser diagnostic set up

OH-LIF is a well-established technique and it is successfully applied for both qualitative and quantitative measurements of turbulent flames. LIF of the OH radical is widely used to mark flame fronts and to allow investigations of the flame front interaction with the turbulent flow field [15, 16]. OH radicals can exist over a large region of space in turbulent flames and indicate the presence of high temperature and hot products of combustion. Sharp OH gradients achieved with LIF allow unambiguous detection of the local flame front position. For this reason, OH-LIF was employed in this study in order to investigate the flame front oscillations. FIG. 2 represents a schematic view of the laser diagnostic set-up.

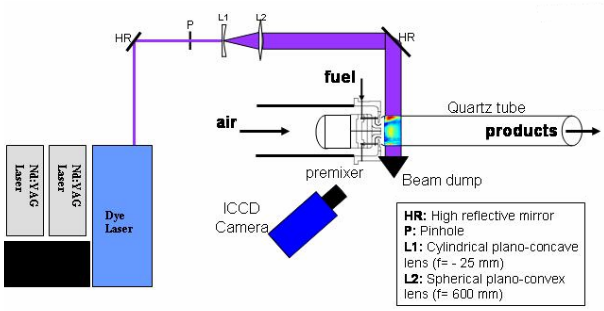

FIG. 2. Laser diagnostic set up

To excite OH, a frequency doubled dye laser (Sirah Cobra-Stretch) using Rhodamine 6G is used. Two Nd:YAG lasers (Continuum Surelite) at λ=532nm output are used to pump the dye laser. The dye laser is tuned to the $Q_1(5)$ transition in the (1,0) band of the OH $A^2\Sigma^+ \leftarrow X^2\Pi$ system at λ_{Exc}=282.75 nm (6 mJ energy per pulse). A light sheet is formed using a -25 mm cylindrical lens (L1) and is focused by a 600 mm spherical lens (L2) to a thickness of approximately 300µm in the center plane of the combustor. It is located adjacent to the front face of the swirler unit and its width is around 45 mm. The fluorescence signal is collected at right angle (side view) with a high resolution ICCD camera (LaVision Nanostar) using a 135mm f/4.5 UV Nikkor lens. A combination of a UG11 and a WG305 filters are used in front of the camera, which allow transmission of the LIF signal, corresponding to emission in the (1,1) and (0,0) bands around λ=310nm.

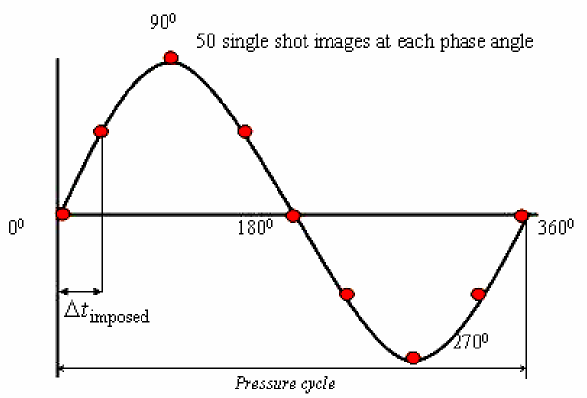

FIG. 3. Pressure cycle with image phase angles

In order to study the local fuel distribution over the pressure cycle Acetone-LIF is applied. The acetone is introduced into to the fuel flow by means of a cyclone seeder. Only gaseous acetone at trace amounts is introduced into the flow. The Acetone-LIF imaging is phase locked to the pressure oscillation in the manner it is in the case of the OH-LIF imaging process. Acetone can be excited in a wavelength range 225 nm<λ_{Exc}<330 nm, with a maximum at $\lambda_{Exc,max}$=278 nm. In these experiments a frequency-quadrupled Nd:YAG laser was used to excite the Acetone at a wavelength of λ_{Exc}=266 nm which is close to the excitation maximum wavelength. The resulting absorption cross section is σ=4.4·10^{-20} cm^2. The acetone molecules change to the first excited singlet state (S_1) from which close to 100% change to the first excited triplet state (T_3) by intersystem crossing. No fluorescence light is emitted from this state. Almost all of the molecules remaining in S_1 then fluoresce emitting radiation in a wavelength range 335 nm<λ_{LIF}<550 nm, with emission maxima at $\lambda_{LIF,max}$=435 nm and $\lambda_{LIF,max}$=480 nm and a resulting fluorescence yield of Φ_{LIF}=0.2% [19, 21]. Respective filters were positioned in front of the collection optics to prevent imaging of Rayleigh scattering.

In reacting flows, problems can arise due to acetone decomposition by pyrolysis and radical attack [18]. Simultaneous measurements of OH and acetone fluorescence have shown that acetone decomposition is not confined to the flame front area as indicated by the OH-LIF images. It was hence decided to restrict the measurements to cold flow conditions and impose the flow oscillations by means of the siren. Under these conditions the Acetone-LIF data can be quantified much more reliably [20]. The measured fluorescence intensity relates to the number density by:

$$\text{(1)} \qquad \frac{N_{Ac}}{N_{Ac}^0} = \frac{I_{Ac}}{I_{Ac}^0} S_\lambda(T)$$

In this equation N and I are the acetone number density and measured fluorescence light intensity, respectively. The superscript “0” indicates the respective values at a defined and therefore known concentration, variables without the superscript indicate values under experimental conditions. S_λ (T) is a correction factor regarding the variation of fluorescence emission with temperature at a specific wavelength which for λ=266 nm is:

$$\text{(2)} \qquad S_\lambda(T) = 0.9 + 0.25\frac{T}{300K} - 0.15\left(\frac{T}{300K}\right)^2$$

Consequently, under the given experimental conditions this factor equals unity and thus fluorescence light intensity can directly be linked to acetone number density when the respective values for a given reference condition (superscript “0”) are known. The reference condition fluorescence intensity is determined by taking a series of images at known stationary mass flows of air, fuel and acetone and thus a known acetone number density. Consequently, it is possible to quantify the acetone fluorescence intensities measured in the experiments.

The external trigger of the laser is synchronized with the camera by the image acquisition and camera control software. By using the measured pressure signal to trigger the laser and the image acquisition process the images can theoretically be locked to any chosen phase angle of the oscillation. In these experiments the complete pressure cycle is resolved into 9 equally spaced phases. This results in coverage of the oscillation cycle from 0° to 360° with a phase angle step width of 45° (FIG. 3). This way 50 images locked to one particular oscillation phase angle are recorded in an experiment.

Due to the nature of the phase locking of the images a phase shift correction with respect to the imaged phase angle has to be performed afterwards. This is necessary since there is a non-negligible distance between the pressure transducer in the combustion chamber to which controls the phase locking of the imaging and the imaged area of interest (AOI). This particular pressure probe is located 700 mm downstream of the swirler front plate. In combination with a 40 mm wide AOI beginning immediately downstream of the swirler front plate, the average distance between the AOI and the pressure transducer is Δl=680 mm (see FIG. 4).

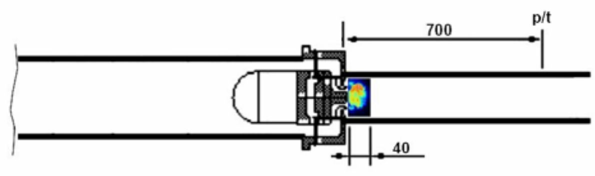

FIG. 4: Distance between pressure transducer (p/t) and AOI

This results in a substantial difference regarding the phase angle measured at the pressure probe and the phase angle of the oscillation present at the AOI at the identical point in time. This difference largely depends on the gas composition and temperature, i.e. on the experimental flow conditions, as well as the frequency of the oscillation. At the Acetone-LIF experiments, flow composition and temperature are known (non-reacting flow, all species at ambient temperature). For the OH-LIF experiments the gas composition is assumed to be the result of the complete combustion of the injected fuel. Previous experiments have shown the average flow temperature downstream of the combustion region to be around T=1100 K. At an oscillation frequency of ν=200 Hz this results in a phase shift of 75° (0.41 π) at reacting flow conditions in the OH-LIF experiments and 141° (0.78 π) in the non-reacting flow Acetone-LIF experiments.

3. RESULTS AND DISCUSSION

3.1. Comparison of OH-LIF of self excited and forced oscillation flames

All images are post processed by camera background subtraction. Both the OH-LIF and the Acetone-LIF images are also corrected by subtracting a specific light sheet image which has been acquired for each respective experiment. This includes also the Acetone-LIF reference images. The OH-LIF images are normalized by the same image to account for energy gradient in the incident laser light sheet. The Acetone-LIF images are normalized by a fluorescence intensity which corresponds to a stoichiometric equivalence ratio, determined from the reference images, thus resulting in direct indication of the local equivalence ratio in each single shot image.

FIG. 5 shows a comparison of OH-LIF single shot images at 200 Hz self excited oscillation versus forced oscillation. OH-LIF can be used to define the boundary between reactants and products. Please note that the OH-LIF images are single shot data, and the colour bar represents OH fluorescence intensity in counts. The images at the various phase angles display a development of the flame extension and location which is quite similar for both cases although not identical. For the self-excited case at some phase angles, the OH-LIF shows a more connected flame boundary in both the upper and lower parts of the flame. This is in contrast to the forced flame, which rather seems to be divided into two half flames on the combustion chamber top and bottom, respectively. The measured OH fluorescence intensity in the center of the combustion chamber is comparatively low, thus the apparent split up into two single flames.

This result could be confirmed by measuring imaged intensities. The basic evolution of the flame throughout the pressure cycle is rather similar in the most prominent respects. Maximums of OH fluorescence intensity occur mostly at the same phase angles in both cases, with only one exception at which the measured maximum in the forced oscillation case is reached 45° after the one in the self excited case. The oscillation cycles in most locations of the AOI are alike. The most striking differences are that in the self excited oscillation case the maximum lies three times as high above the average recorded intensity value as compared to the forced oscillation case while the average intensity in many locations of the AOI is comparable and that there is a substantial fluctuation of OH fluorescence intensity in the center of the AOI in the self excited oscillation case while this effect is only exhibited to a minor degree in the forced oscillation case.

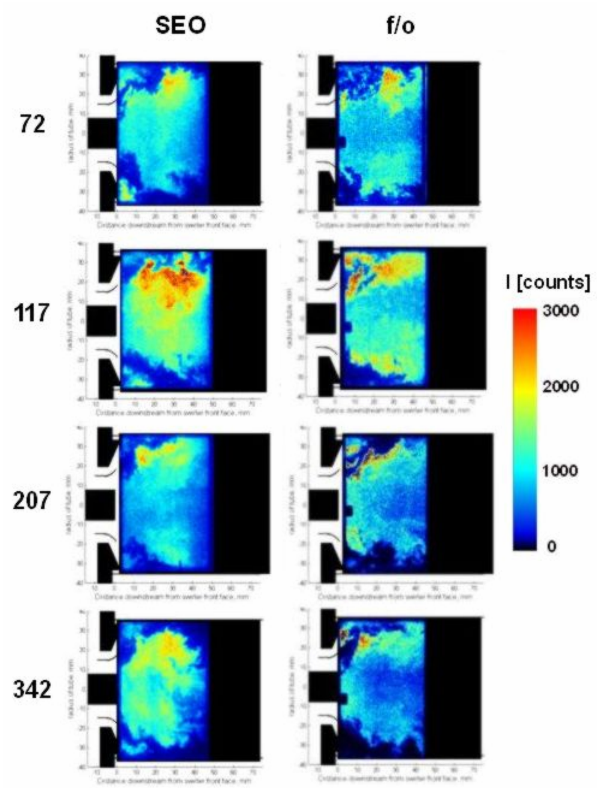

FIG. 5: OH-LIF intensities (scale in counts); comparison of self excited oscillation (SEO) vs. forced oscillation (f/o) at various phase angles (top to bottom, phase angles in degrees are indicated on the left)

3.2. Comparison of oscillation cycles of OH-LIF and Acetone-LIF/equivalence ratio

By means of the Acetone-LIF reference images, the images acquired during the experiments can be converted into images showing the oscillation of local equivalence ratio distribution over the pressure cycle (see FIG. 7). These images show how the fuel enters the combustion chamber in jet like features, especially at phase angles 226°, 271° and 316°. The average equivalence ratio appears to be relatively high, i.e. above the overall equivalence ratio of the entire flow of Φ=0.6, in two areas between the center and the top and bottom wall of the combustion chamber, respectively.

To extract quantitative data from both equivalence ratio and OH-LIF images, rectangles have been defined on the AOI in which statistical data could be determined (see FIG. 6).

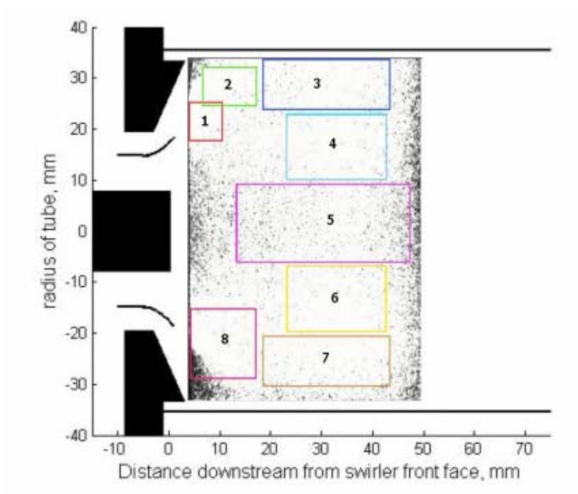

FIG. 6: Rectangles in AOI for data extraction

The designations of these recangles are as follows:

1 – jet top left
2 – jet top right
3 – rear top
4 – rear high
5 – center
6 – rear low
7 – rear bottom
8 – jet bottom

The area where the upper fuel jet enters the combustion chamber has been split into 2 rectangles (compared to the corresponding area on the bottom) to capture this area in better detail. The so acquired values for average intensities of OH fluorescence intensity or local equivalence ratio can then be plotted parallel in one diagram (see FIG. 8 and 9).

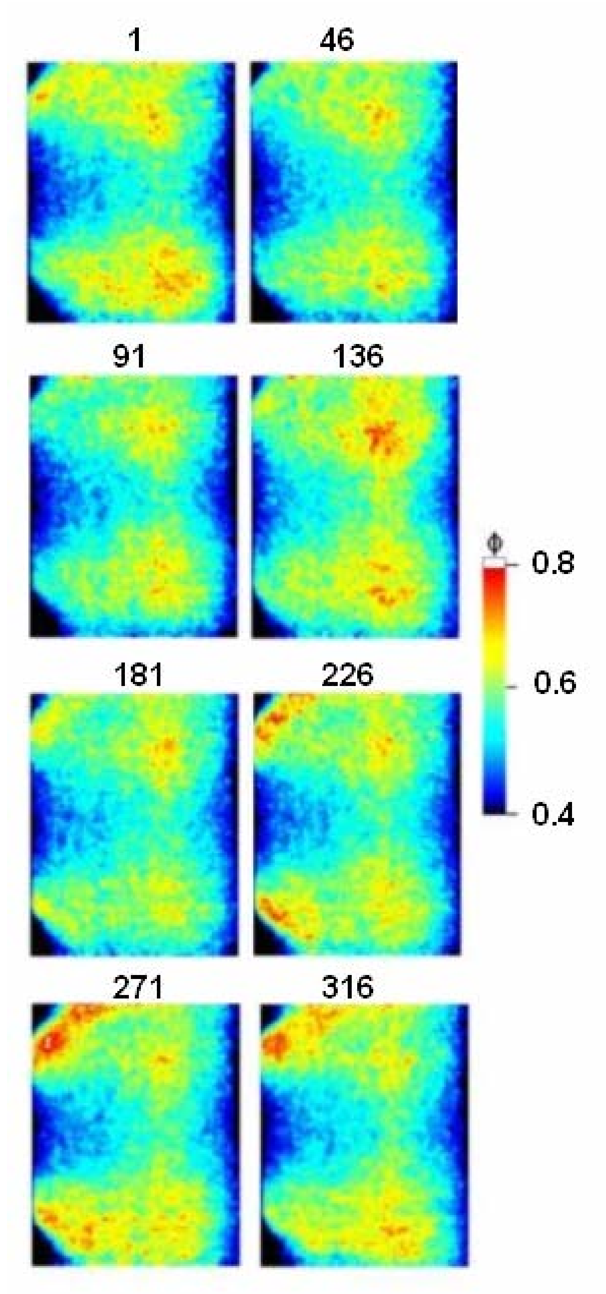

FIG. 7: Fluctuation of local equvalence ratio during one oscillation cycle, numbers above image indicate phase angle

The plots in FIG. 8 and 9 represent the true numerical values of local equivalence ratio (lower set, marked by circles) while the values for OH-LIF intensity are displayed in arbitrary units (upper set, marked by triangles). OH-LIF data originate from self excited oscillation experiments. Both plots show a similar trend: While there is a substantial fluctuation of the OH-LIF intensity in all measured areas of the AOI, the equivalence ratio only shows major fluctuations in the fuel jet areas. The lag between the peaks of OH-LIF intensity and local equivalence ratio at both the top and bottom fuel jet areas is approximately 145°. The evolution of the measured equivalence ratio is in accordance with the change of the average flow velocity based on changes in static pressure during the oscillation. As the phase angle passes 180°, the pressure decreases below average, approaching its minimum value, while the overall flow velocity approaches its maximum. Consequently, as the flow through the swirler and the AOI is increasing more fuel is injected into the combustion chamber. The increased amount of fuel injected from the swirler may also result from the phase of lower flow velocity through the swirler. During this phase of the flow, fuel could possibly accumulate inside the swirler to a certain degree, since fuel injection is unaffected by the conditions prevailing at the respective point (choked flow). As the pressure rises again the fuel injection appears to return to some average amount slightly varying between Φ=0.6 and Φ=0.55.

One area not representing a fuel jet but still showing prominent changes of Φ is the one designated ‘rear bottom’ (rectangle 7). It is particularly interesting that the equivalence ratio in this specific rectangle pretty much remains constant from 46° to 181° phase angle, as is the case at the area ‘rear low’ (rectangle 6). Judging from looking at the pictures alone, it seems that the equivalence ratio would continue to decrease past a phase angle of 46°. But the measurement shows that this is not the case. Be aware that the higher curvature of some of the plots which are represented in FIG. 9 as well results from the different scale on the y-axis.

So by visual impression the equivalence ratio seems to decrease but the measurements show it to be rather constant. This indicates that only the visually more obvious spots of locally scattered relative peak values of Φ within this area disappear but the fuel essentially stays there. This happens while the pressure at the AOI is rising and the overall flow velocity decreasing. At this stage the fuel is most likely being caught in a recirculating vortex which increases the residence time and enhances small scale mixing, resulting in a uniform distribution of fuel. This sequence of increased fuel injection, accumulation and enhanced mixing in a potential recirculation zone is also in rather good accordance with the OH-LIF results.

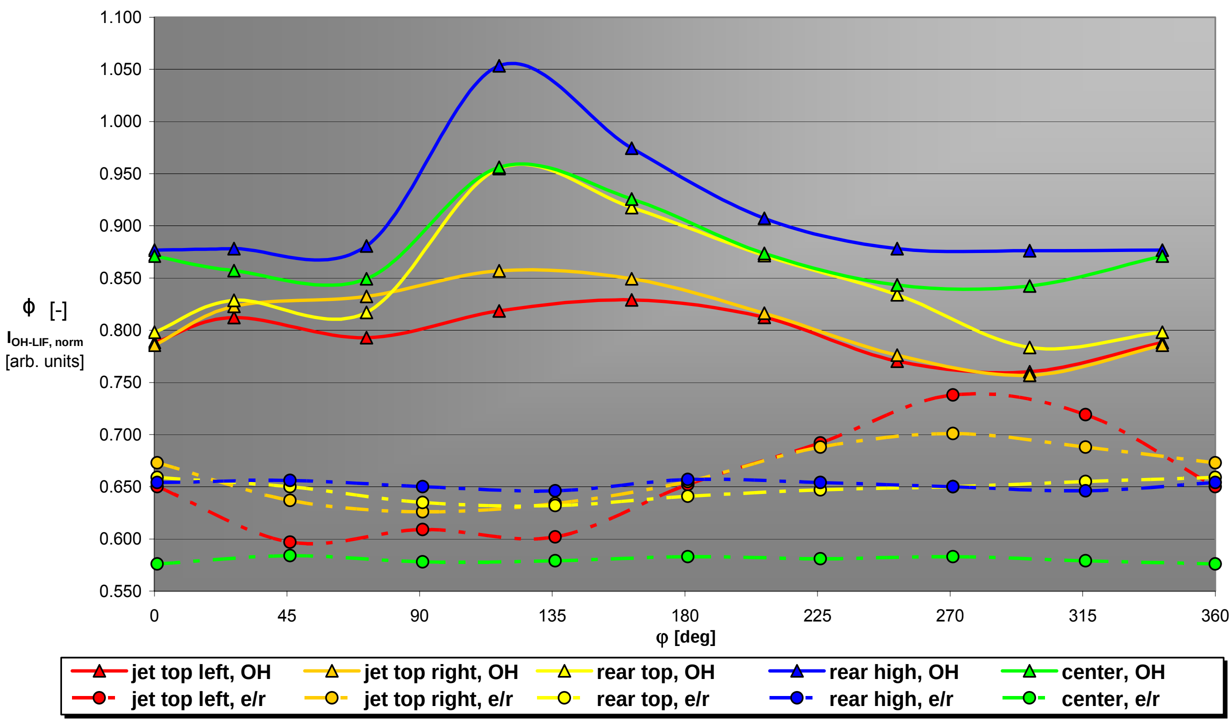

FIG. 8: OH-LIF intensity and equivalence ratio (e/r), combustion chamber top half

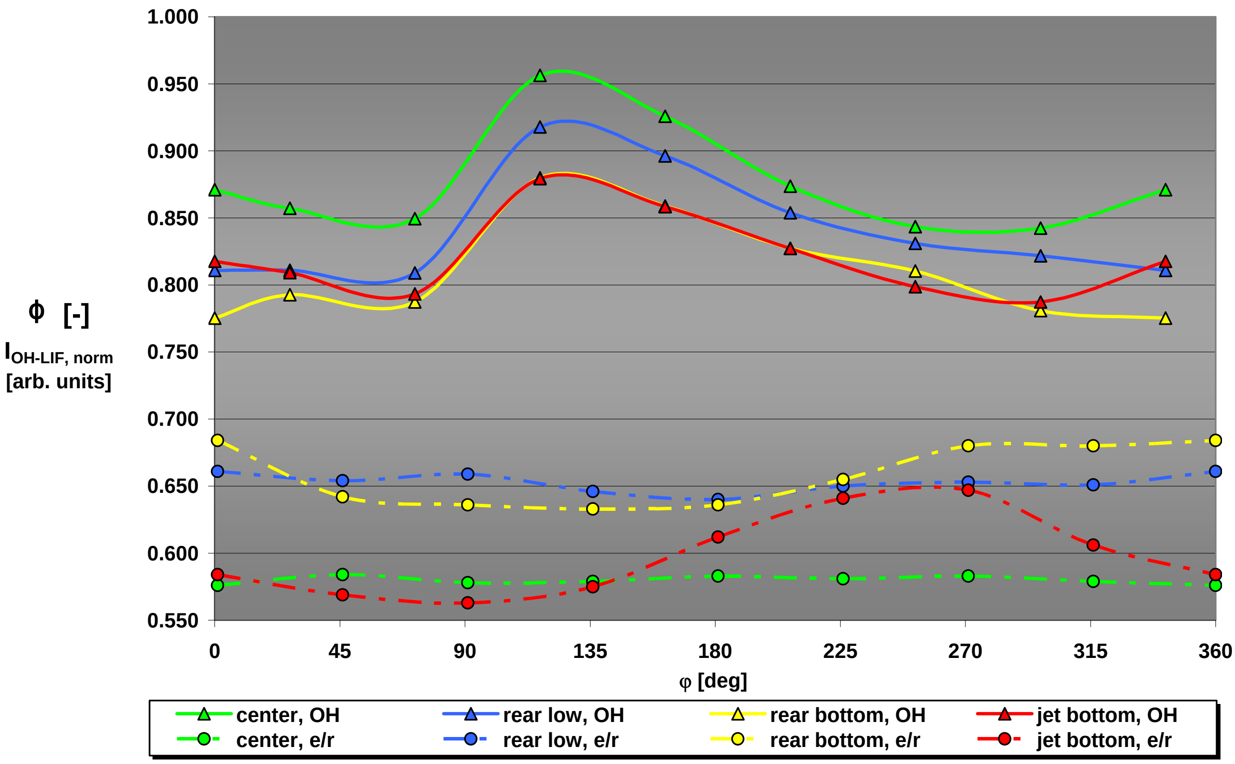

FIG. 9: OH-LIF intensity and equivalence ratio (e/r), combustion chamber bottom half

Based on these the combustion maximum is measured at a phase angle which lies in that part of the pressure cycle where the small scale mixing enhancement may be in effect thus favouring high rates of combustion (see figure 14). The fact that the measured local equivalence ratio remains high must be attributed to the fact that Acetone LIF experiments are carried out under cold flow conditions.

4. CONCLUSIONS AND FUTURE WORK

Based on OH-LIF intensity there is a distinctive increase in the flame front surface area and combustion intensity during the peaks of the self excited oscillations. This increase can be observed at forced oscillations at the same phase angles as well but to a much lesser extent. Since the pressure perturbation generated by the siren is not as intense as the one observed in the the self excited oscillation case, apparently this forcing can not cause according fluctuions of this magnitude. Since the forced oscillation nevertheless seemms to simulate the overall flow condition during the pressure cycle reasonably well, conclusions can also be drawn from the quantified Acetone-LIF experiments, even though these are carried out in non-reacting flow conditions.

There appears to be a substantial influence of the local phase angle of the acoustic wave in the combustion chamber and its associated velocity fluctuations. This seems to allow for build up of local equivalence ratio maxima both in the inlet duct of the swirler and in potential recirculating vortices. This results in temporarily present relatively fuel rich and well mixed areas. This mechanism is confirmed by the fact that the phase angle at which these areas can be observed is near those with maximum OH-LIF intensities at the respective areas.

For further quantitative data analysis flame curvatures and flame surface densities are presently being determined from the OH-LIF images. This should give a more detailed understanding of the propagation of the flame while building up to its maximum and its break down while it decreases and sometimes even experiences local extinction.

Also the results from identical experiments at other oscillation frequencies and at AOIs outside of the combustion chamber's center plane will be included to get a more complete understanding of the dynamic processes in the combustion chamber.

Acknowledgement

This work has been funded by the EU's Sixth Framework Programme INTELLECT D.M. contract (EU Project AST3-CT-2003-502961, Jan 01, 2004 - Dec 31, 2007). The authors also wish to thank Rolls Royce plc.; Miss Gashi expresses her thanks to EPSRC for the CASE award, and Mr Kaminski to the Leverhulme trust for personal funding and to EPSRC for the PLATFORM grant.

5. REFERENCES

1. Dowling, A.P.: "The calculation of thermoacoustic oscillation", *Journal of Sound and Vibration*, 180, 557-581, 1995
2. Paschereit, C. O., Gutmark, E. and Weisenstein, W.: "Structure and control of thermoacoustic instabilities in a gas turbine combustor", *Combustion Science and Technology*, 138: 213-232, 1998
3. Kelsall, G. and C. Troger: "Prediction and control of combustion instabilities in industrial gas turbines", *Applied Thermal Engineering*, 24, 2004
4. Dowling, A.P. and Stow, S.R.: "Acoustic analysis of gas turbine combustors", *Journal of Propulsion and Power*, 19 (5) 751-764, 2003
5. Dowling, A.P.: "Thermoacoustic instability", 6^{th} International Congress on Sound and Vibration, 3277-3292, 1999
6. Armitage, C. A., Riley, A.J., Cant, R.S., Dowling, A.P. and Stow, S.R.: "Flame transfer function for swirled LPP combustion from experiments and CFD", Asme Turbo Expo 2004, 2004-GT-53820, 2004
7. Rayleigh, Lord: "The theory of sound", London, Macmillan, 1986
8. Bloxsidge, G.J., Dowling, A.P. and Langhorne, P.J.: "Reheat buzz: An acoustically coupled combustion instability, Part 2. Theory", *Journal of Fluid Mechanics*, 193, 445-473, 1988
9. Zhu, M., Dowling, A.P. and Bray, K.N.C.: "Self-excited oscillations in combustors with spray atomisers", ASME 2000-GT-108, 2000
10. Richards, G. A. and M. C. Janus: "Characterization of oscillations during premix gas turbine combustion", ASME 120: 294-302, 1998
11. Paul, P. H. and Najm, H. N.: "Planar Laser-Induced Fluorescence Imaging of Flame Heat Release Rate", Proc. Comb. Inst., 27, 43-50, 1998
12. Ayoola, B. O., Balachandran, R., Frank, J.H., Mastorakos, E. and Kaminski, C.F. : "Spatially resolved heat release rate measurements in turbulent premixed flames", *Combustion and Flame*, 144: 1-16, 2005
13. Riley, A., Park, S., Dowling, A.P., Evesque, S. and Annaswamy, A.M.: "Adaptive closed-loop control on an atmospheric gaseous lean premixed combustor", Asme Turbo Expo 2003, GT-2003-38418, 2003
14. Englund, D.R., Richards, W.B., Proc. 30th International Instrumentation Symposium, May 7-10 Denver CO, pp. 115-124, 1984
15. Kaminski, C. F., Bai, X.S., Hult, J., Dreizler, A. Lindenmaier,S. and Fuchs, L.: "Flame growth and wrinkling in a turbulent flow", *Applied Physics*, B 71: 711-716, 2000
16. Kaminski, C.F., Hult, J., Richter, M., Nygren, J., Franke, A. and Alden, M: "Development of high speed spectroscopic imaging techniques for the time resolved study of spark ignition phenomena", SAE 2000-01-2833, 2000
17. Lawn, C. J.: "Distribution of instantaneous heat release by the cross correlation of chemiluminescent emissions", *Combustion and Flame*, 123: 227-240, 2000
18. Yip, B.; Miller, M.F.; Lozano, A.; Hanson, R.K.: "A combined OH / Acetone planar laser-induced fluorescence imaging technique for visualizing combusting flows", *Experiments in Fluids*, 17 (1994), pp. 330-336, Springer-Verlag 1994
19. Lozano, A.; Yip, B.; Hanson, R.K.: "Acetone: a tracer for concentration measurements in gaseous flows by planar laser-induced florescence", *Experiments in Fluids*, 13, pp. 369-376, Springer-Verlag 1992
20. Bryant, R.A.; Driscoll, J.F.: "Structure of Supersonic Flames Imaged Using OH/Acetone Planar Laser-Induced Fluorescence", *AIAA Journal*, Vol. 39, No. 9, September 2001
21. Bunyajitradulya, A.; Papamoshou, D.: "Acetone LIF Imaging of Turbulent Shear-Layer Structure at High Convective Mach

Number", AIAA 94-0617, 32nd Aerospace Sciences Meeting & Exhibit, Reno, Nevada, USA, 10-13 January 1994